

Article

The Advances and Challenges of the Ediacaran Fractured Reservoir Development in the Central Sichuan Basin, China

Xiao He ¹, Guian Guo ¹, Qingsong Tang ¹, Guanghui Wu ^{2,*}, Wei Xu ¹, Bingshan Ma ² , Tianjun Huang ¹ and Weizhen Tian ²

¹ PetroChina Southwest Oil & Gasfield Company, Chengdu 610051, China

² School of Geoscience and Technology, Southwest Petroleum University, Chengdu 610500, China

* Correspondence: wugh@swpu.edu.cn

Abstract: The largest Precambrian gasfield in China has been found in the central Sichuan Basin. It has been assumed as an Ediacaran (Sinian) mound–shoal, microfacies-controlled, dolomite reservoir. However, the extremely low porosity–permeability and heterogeneous reservoir cannot establish high production by conventional development technology in the deep subsurface. For this contribution, we carried out development tests on the fractured reservoir by seismic reservoir description and horizontal well drilling. New advances have been made in recent years: (1) the prestack time and depth migration processing provides better seismic data for strike-slip fault identification; (2) seismic planar strike-slip structures (e.g., en échelon/oblique faults) and lithofacies offset together with sectional vertical fault reflection and flower structure are favorable for strike-slip fault identification; (3) in addition to coherence, maximum likelihood and steerable pyramid attributes can be used to identify small strike-slip faults and for fault mapping; (4) fusion attributes of seismic illumination and structural tensor were used to find fractured reservoir along fault damage zone; (5) horizontal wells were carried out across the strike-slip fault damage zone and penetrated fractured reservoir with high production. Subsequently, a large strike-slip fault system has been found throughout the central intracratonic basin, and the “sweet spot” of the fractured reservoir along the strike-slip fault damage zone is widely developed to be a new favorable domain for high-production development. There is still a big challenge in seismic and horizontal well technology for the economical exploitation of the deep fractured reservoirs. This practice provides new insight in the deep tight matrix reservoir development.



Citation: He, X.; Guo, G.; Tang, Q.; Wu, G.; Xu, W.; Ma, B.; Huang, T.; Tian, W. The Advances and Challenges of the Ediacaran Fractured Reservoir Development in the Central Sichuan Basin, China. *Energies* **2022**, *15*, 8137. <https://doi.org/10.3390/en15218137>

Academic Editors: Junqian Li, Wenhao Li and Reza Rezaee

Received: 31 August 2022

Accepted: 12 October 2022

Published: 1 November 2022

Publisher’s Note: MDPI stays neutral with regard to jurisdictional claims in published maps and institutional affiliations.



Copyright: © 2022 by the authors. Licensee MDPI, Basel, Switzerland. This article is an open access article distributed under the terms and conditions of the Creative Commons Attribution (CC BY) license (<https://creativecommons.org/licenses/by/4.0/>).

1. Introduction

With the exhaustion of the hydrocarbon resources in the Meso-Cenozoic strata, the ancient Precambrian reservoir has been becoming a potential domain in oil/gas exploration and development [1,2]. Precambrian petroleum systems and their oil/gas resources have been discovered in East Siberia, North Africa, the Middle East, North America, India and Central and South America [1–6]. Owing to multiple structural and diagenetic activities in the deeper subsurface, the ancient Precambrian oil/gas resources at the base of petrolierous basins are generally characterized by complicated accumulation and production. Subsequently, they had more difficulties in the Precambrian oil/gas resource exploration and development, as well as much less oil/gas production from the ancient strata [1–6]. In recent years, Neoproterozoic continental rifts have been found in the Sichuan, Tarim and Ordos basins in China [7–9]. Furthermore, the giant Anyue Gasfield has proven geological reserves more than $1 \times 10^{12} \text{ m}^3$ in the Ediacaran–Cambrian dolomite, indicating huge exploitation potential of deep Precambrian carbonates [10–12]. Since then, the Precambrian reservoir has consequently become an important exploitation frontier in China.

In the Anyue Gasfield, the late Ediacaran mound–shoal bodies widely developed along the platform margin and in the interior platform [13,14]. The reservoir mainly occurred in the high-energy mound–shoal dolomite, which is generally thought to be the major controlling factor on the carbonate reservoir [12–15]. It is assumed that the arid paleoclimate was favorable to develop the primary matrix pore-type reservoir in the mound–shoal bodies [15]. Recent studies revealed an unconformity and distinct karst process by the Precambrian Tongwan movement in the central uplift [15–17]. They showed that most porosity in the Ediacaran is secondary dissolution porosity. These studies suggested that the karstification before the Cambrian deposition has resulted in a large amount of dissolution pores and vugs in the Dengying Formation, which had complicated diagenesis and origin during the long burial history [12,16,17]. The Precambrian karstification led to a widespread development of dissolution pores, vugs and caves in the carbonate reservoirs. Recently, a lot of exploitation work has been deployed in the deep ancient carbonate reservoirs [10]. However, the Ediacaran reservoirs are quite different from the carbonate reservoirs of high primary porosity in the Meso-Cenozoic. They generally have low porosity (<4%) and permeability (<1 mD) and intense heterogeneity for low production. The production data show that conventional methods and technologies are not enough to efficiently exploit the large number of reserves from the deep Precambrian reservoirs. Recent studies showed that strike-slip faults developed in the central Sichuan Basin [18–20]. These faults resulted in the variable and complicated sedimentary microfacies of the Ediacaran carbonates [20]. In addition, the fault network could connect source rock and enhance porosity and permeability for high production in the deep Ediacaran carbonate reservoirs [19]. However, it is ambiguous if there is large-scale fractured reservoir in the deep subsurface and little information on the exploitation of this kind reservoir.

For this contribution, we present recent advance in seismic technology on the strike-slip fault mapping and fractured reservoir description in the Anyue Gasfield. Based on the geological and geophysical data, we propose a method and its result on horizontal well drilling across different fault zones to explore the Ediacaran fractured reservoir. Furthermore, we discuss the challenge in the fractured reservoir exploitation technology in the deep ancient carbonate.

2. Geological and Exploitation Background

The Sichuan Basin covers an area more than 560,000 km² in southwestern China [21]. It is a superimposed basin with complete Ediacaran–Cenozoic strata that has recorded the opening–closing cycles of the Proto- to Neo-Tethys oceans [21,22]. The basin developed Ediacaran post-rift successions in the pre-Ediacaran metamorphic basement. The Lower Ediacaran Doushantuo Formation deposited thick sandstones and interbedded mudstones and progressively turned to dolomites in an intracratonic shelf environment. The Upper Ediacaran Dengying Formation composed of two sets of thin shale–thick dolomite assemblages in the central carbonate platform (Figure 1) [12–14]. In the end of the Ediacaran, the central Sichuan Basin had a regional uplift and subsequent unconformity karstification [15]. A N–S-trending Deyang–Anyue intracratonic rift trough developed to the western Anyue Gasfield, which is unconformably filled with the Lower Cambrian shales. Thick Cambrian–Ordovician carbonates were deposited in succession in the intracratonic basin. At the end of Silurian, the central uplift formed with the absence of the Silurian–Carboniferous by a regional compressional tectonic movement. During the Permian–Middle Triassic, the carbonate platform developed widely and was then overlain by the late Triassic–Cretaceous siliciclastic deposition in the central basin. With the progressively increased Indo-Asian collision in the Cenozoic, the western foreland depression took shape, and multiple thrust fault systems developed around the basin margins [21,22]. During the multiple tectono-sedimentary evolution, a broad and inherited central paleo-uplift developed in the central intracratonic basin.

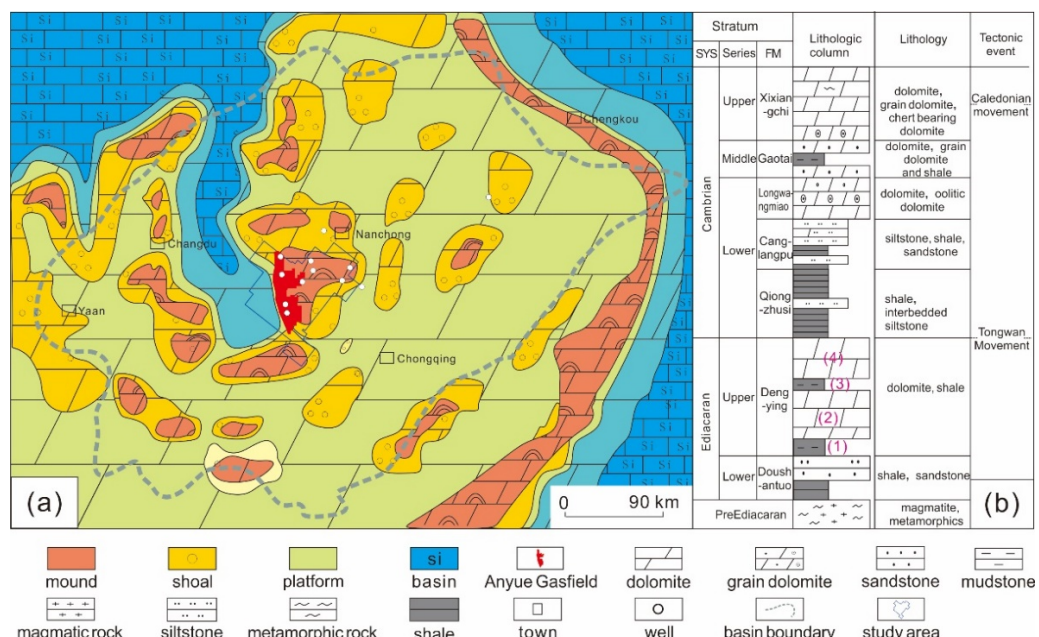


Figure 1. (a) The paleogeographic map of the Ediacaran Dengying Formation and (b) the stratigraphic column of the Ediacaran–Cambrian in the Sichuan Basin ((1)–(4): four members of Dengying Formation; SYS: System; FM: Formation; revised from references [20]).

The Anyue Gasfield is composed of two large anticline traps with a large area of 7500 km² in the central Sichuan Basin (Figure 1) [10,23]. The source rocks are mainly of shales from the Lower Cambrian Qiongzhushi and some from the Ediacaran Dengying and Doushantuo formations [23–25]. The carbonate rocks and the overlain shales formed favorable source–reservoir–cap assemblage. Generally, the oil accumulation occurred in the Permian–Early Triassic and subsequent cracked gas accumulation in the late Triassic–Jurassic during the rapid subsidence in the central basin [23–25]. The burial depth of the Ediacaran reservoir is up to 5000~5500 m. The formation temperature is much higher, up to 145~160 °C, and the formation pressure is in the range of 56~59 mPa with a pressure coefficient of 1.07~1.09. The fourth member of the Dengying Formation is the major reservoir interval that is mainly of microbial dolomite and grain dolomite. There are multiple reservoir layers with a single-layer thickness varied in the range of 1~40 m. The reservoir spaces are mainly of dissolution microbial pores, interparticle dissolution pores and vugs [12,15–17]. It is noted that some wells have penetrated fractures and show much higher permeability and production. The reservoirs can be divided into pore-type, vug-type and fracture–vug-type. The porosity and permeability of the matrix reservoirs are variable in a large range to show strong heterogeneity, and their average values are less than 4% and 0.5 mD, respectively. The absolute open flow of a gas well is varied at $(2\sim 531) \times 10^4$ m³/d, and more than 70% of wells are less than 30×10^4 m³/d. This suggests that the deep burial gas reservoir is characterized by multiple thin layers, complicated tri-pore media, extremely low matrix porosity and permeability, strong heterogeneity, high temperature and pressure and varied production.

For the large-scale gas development of the fourth member of the Dengying Formation in the Anyue Gasfield, a series of technologies have been used in the gas reservoirs [10,23]. The high porous blocks were optimized for development by the reservoir modeling and seismic description in the karstic reservoirs. As a result, the reservoir encounter rate has increased more than 26%. On the production reserve evaluation in the strong heterogeneous reservoirs, the gas recovery of different reservoirs has been evaluated to optimize favorable reservoir targets. Furthermore, the drilling technology has been optimized in the strong heterogeneous reservoirs. The highly deviated well is deployed in multiple superimposed reservoirs and a horizontal well with a horizontal section of 800–1100 m has been deployed

in lateral connected reservoirs. In addition, the well spacing between horizontal wells were adjusted by the reservoir quality. Subsequently, the ratio of drilling failure decreased from 20.7% to 4.9%, and the reservoir penetration rate increased from 24.2% to 87.3%. In addition, the variable acid fracturing process in different segments has been carried out to increase gas production in strong heterogeneous reservoirs in the highly deviated and horizontal wells. With the advances in the development technologies, the annual gas production has been enhanced to more than $60 \times 10^8 \text{ m}^3$ in the fourth member of the Dengying Formation [10]. However, there are still many low-production wells that have big challenges in “sweet spot” reservoir prediction to obtain economic benefit in the deep subsurface.

3. Discovery of a Large Strike-Slip Fault System

3.1. Seismic Data Processing

A 3D seismic survey of more than $22,000 \text{ km}^2$ has been carried out in the central Sichuan Basin (Figure 1). The seismic data are favorable for the strata interpretation of the top and base of the Dengying Formation. As the seismic data are low-resolution with a main frequency of 20–40 Hz, it is hard to identify the strike-slip fault with vertical throw less than 20 m, and it is difficult to describe the dolomite reservoir in the deep subsurface [18,19]. This is shown by the absence of seismic image of the fault plane and lack of fault response in chaotic seismic reflection in the basement. For this contribution, the pre-stack time and depth migration processing has been performed in the 7066 km^2 3D area of the Anyue Gasfield (similar processes in references [23,26]).

In the prestack time migration process, a prestack high-fidelity process, well-controlled deconvolution process and multi-information velocity modelling are used to eliminate noise and enhance the imaging effect. Well-controlled TAR factor compensation, grid tomographic velocity update, azimuthal anisotropy correction and post-migration multi-wave suppression have been used in the prestack depth migration process. As a result, the strike-slip fault zone presents distinct vertical flexural deflection or clear fault planes in its seismic section (Figure 2). The weak seismic response of the strike-slip fault could be enhanced, and the deep noises could be eliminated to show clear vertical fault zones in the deep strata. In addition, the reprocessing could improve the seismic image of small faults and fault linkages. Through the seismic processing, some continuous seismic reflections of the vertical flexural deflection could be offset by fault planes or chaotic reflections to indicate strike-slip faults. In this way, the seismic reprocess can improve the fault image accuracy.

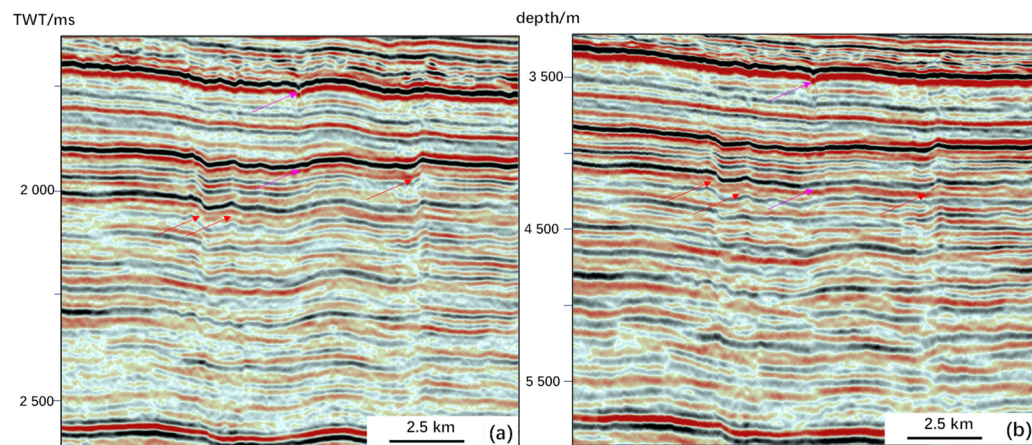


Figure 2. Seismic sections by (a) prestack time migration and (b) prestack depth migration processes in Anyue Gasfield (the red arrows indicating strike-slip fault; the pink arrows showing false image could be inferred to be strike-slip fault).

Furthermore, the process could eliminate some false images showing “strike-slip fault” resulting from the varied velocity of the Triassic evaporates, etc. For example, an

assumed strike-slip fault in the center of Figure 2 could be excluded by the reprocessed sections that show continuous antiform reflection rather than chaotic reflection in the unprocessed section. The seismic data are helpful to exclude false fault images of basement fold (Figure 2), fault detachment fold and the velocity pull-up effect by evaporite. In addition, the prestack seismic reprocessing could provide better seismic attributes in strike-slip fault identification. The prestack seismic process could improve fault resolution which could be very helpful in small fault identification (Figure 3). In addition, the fault image by prestack depth migration process could be better than the prestack time migration. In this way, the prestack time/depth migration process provides higher-resolution seismic data for strike-slip fault identification and description in the Ediacaran reservoirs.

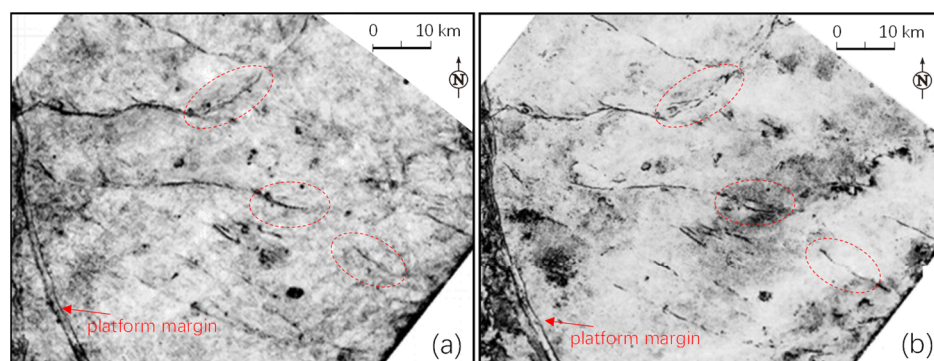


Figure 3. Seismic coherence attribute at top of the Ediacaran by (a) prestack time migration and (b) prestack depth migration processes in Anyue Gasfield (the red circles indicating the prestack depth migration process is better in small strike-slip fault image).

3.2. Identification of Strike-Slip Fault

Generally, the small vertical displacement (<60 m) cannot show obvious slip surface in the seismic section (Figure 2). In this way, vertical flexural chaotic reflection and a flower structure could be used to identify strike-slip fault in seismic section (Figures 2 and 4a). Moreover, the varied height difference of the vertical deformation zone in different strata could be used to identify strike-slip faults. As many seismic sections have an ambiguous fault response in the deep basement, it is hard to distinguish a downward steep strike-slip fault (Figure 4a). In this way, it is generally inferred from the high steep antiform or syncline [18,19]. However, the fault could turn into a small dip to show normal or reverse faults. Furthermore, many more vertical flexural deformations and chaotic reflections could be led by the fold deformation or velocity variation (Figure 3). In addition, the flower structure and high steep fault are not sufficient for strike-slip fault identification, but are pitfalls in misinterpretation [27]. Owing to many false fault images showing in seismic section, they need to be excluded during the seismic section interpretation. The fault properties cannot only be determined by a few profiles, and the interpretation of seismic profile data needs to be carefully discriminated.

On the other hand, typical planar strike-slip structures, such as en échelon/oblique faults and lithofacies offset can be used to identify strike-slip fault [19,27]. Generally, the small strike-slip fault zones present en échelon/oblique faults on coherence and amplitude attributes in Anyue Gasfield (Figures 3 and 4b). These faults are generally associated with brachyanticline or dome structures or minimal pull-apart graben. These are favorable for strike-slip fault identification. In addition, the vertical throw is variable along the fault zone. This is consistent with the segmented fault zone [19]. In the east of this study area, a few fault zones have horsetail faults that can also indicate strike-slip faults. In this context, the planar marks other than section marks are favorable for identifying strike-slip faults in the deep subsurface. The reprocessed seismic data provide more accurate planar attributes for identifying and mapping the strike-slip faults in the deep subsurface. Together with seismic section interpretation, the coherence, curve and coherence-enhancing attributes can be used to map the large strike-slip fault zone (Figures 3 and 4). Owing to the complexity

and diversity of strike-slip faults, it is also needed to exclude the pitfalls in planar strike-slip fault interpretation and mapping.

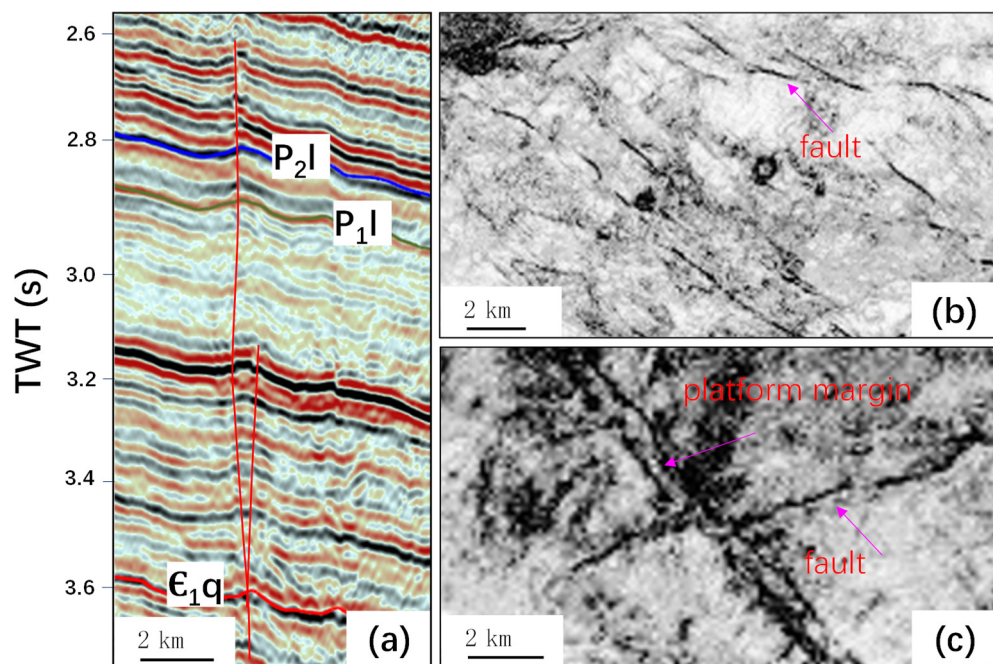


Figure 4. Typical marks of the strike-slip fault in seismic section: (a) vertical plane and flower faults at the lower part) and seismic planar coherence attribute; (b) en échelon/oblique faults; (c) NW-trending platform margin offset by NEE-trending strike-slip fault).

A series of large strike-slip fault zones were identified by seismic sections and coherent attributes. However, the small vertical strike-slip fault generally cannot be identified in the seismic section and is ambiguous in planar attributes. Except for seismic coherence data, maximum likelihood is used to identify the small strike-slip fault. The maximum-likelihood attribute can be used to detect the maximum probability and appropriate location of faults by scanning the fracture similarity in the 3D seismic data [28]. Compared with the conventional seismic attributes of coherence and curvature, the maximum-likelihood attribute can improve the seismic image of small faults and fault segments (Figure 5a,b). It has been shown that the secondary faults are more distinct in the maximum-likelihood attribute. The fault zone is composed of a series of small secondary faults. Furthermore, the steerable pyramid process can be used to image the strike-slip fault [29,30]. The coherence attribute processed by a steerable pyramid could improve strike-slip fault images by suppressing the influence of other geological factors, such as rivers, reef-shoal facies, etc. (Figure 5c,d). The result (Figure 5d) shows distinct fault segments and clear fault traces, which is helpful for small fault mapping and fault linkage analysis. Compared with conventional seismic attributes of coherent and curvature, maximum-likelihood and steerable pyramid attributes can enhance the seismic imaging effect of small faults and fracture assemblages and are helpful in the description of small fault zones.

Together with these methods, the strike-slip faults could be better distinguished in the seismic section and planar map. In this way, a large strike-slip fault system has been found in the 3D seismic area (Figure 6). There are 12 first-order faults with a total length of 860 km, and 13 second-order faults with total length of 630 km in the Ediacaran Dengying Formation. Most strike-slip faults present as NWW-trending across the study area. In addition, some smaller NE-trending strike-slip faults have been found in the 3D seismic area. Generally, the first-order fault zone is more than 50 km in length and more than 60 m in vertical displacement, as well as a fault damage zone width of more than 1 km. The associated third-order faults developed along the major first and second faults or among them. They are generally isolated en échelon or oblique assemblages at the top

of the Ediacaran carbonate. These fault network form a large number of faulted blocks throughout the 3D area. The major strike-slip faults are inherited upward to the Cambrian, and some extend to the Permian and Triassic. They show multiple flower structures in different strata to show multi-stage fault activities.

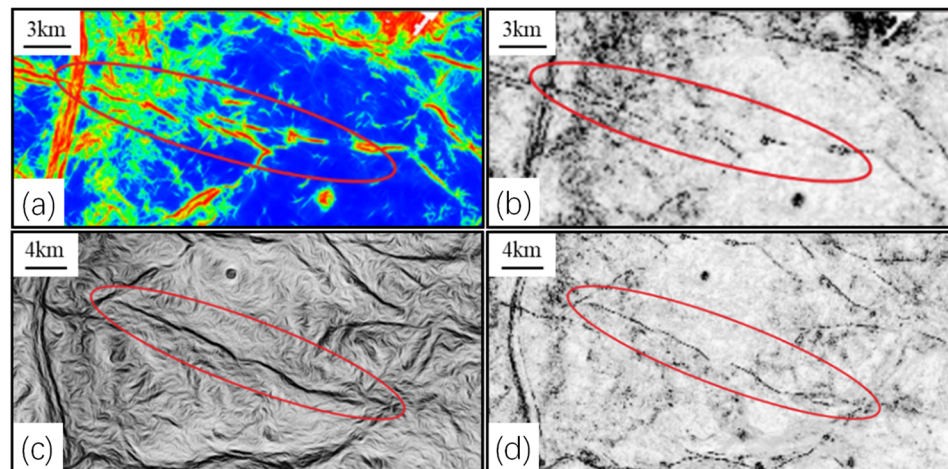


Figure 5. Comparison of (a) the planar maximum likelihood attribute and its counterpart of coherence attribute (b), and (c) coherence attribute and (d) its steerable pyramid process in imagining the strike-slip faults in Anyue Gasfield (the red circle highlighting the comparison images of the fault network).

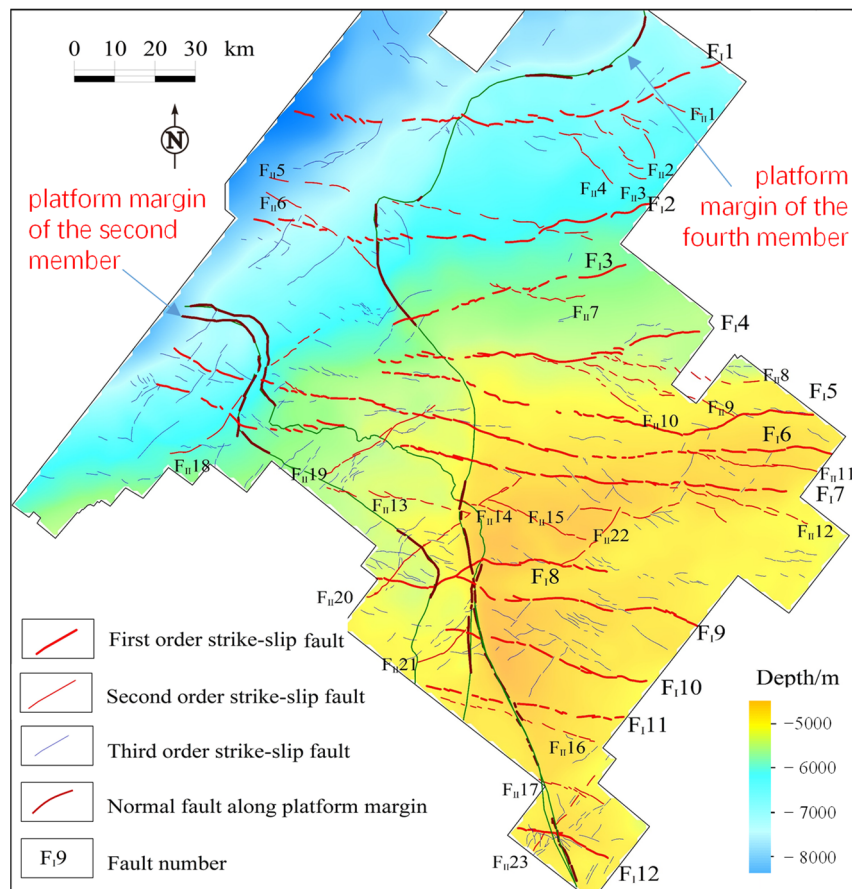


Figure 6. The strike-slip fault system at the Ediacaran Dengying Formation in the central Sichuan Basin (the first order strike-slip fault zone could extend out of the 3D area and offset across the platform margin of the Dengying Formation; after reference [20]).

4. Advance in Fractured-Reservoir Exploitation

4.1. Description of Fractured Reservoir

Generally, it is hard to describe the small-scale fracture and fractured reservoirs in the deep subsurface [31–33]. Owing to the fracture and fractured reservoirs often occurred in the fault damage zone, we use seismic illumination attribute to constrain the envelope of the fault damage zone and the fracture-cave reservoirs. The seismic illumination process is based on the analysis parameters of illumination energy that are favorable for improving the imaging accuracy of seismic data in complex structures (the method based on references [34,35]). In addition, we use attribute fusion by structural tensor attribute (similar method to reference [33]) to improve the images of the fault damage zone and the fractured reservoirs. Using well calibration, the fusion of these attributes was performed to distinguish the fracture network and fractured reservoirs from the surrounding rocks.

Compared with conventional coherence attributes, this method can image better architecture of the fault damage zone (Figure 7). The fault line, but not the boundaries of the fault damage zones, can be defined in the coherence attribute (Figure 7a). Using the seismic illumination process, the fault damage zones could be imaged along the fault zone (Figure 7b). Furthermore, the attribute fusion is carried out by the structural tensor process on the seismic illumination attribute. In this way, there is a distinct image of the fault damage zone (Figure 7c). The fault core generally shows a strong structural tensor with symmetrical damage zones on both sides. The intensity of the fault damage zone suggests the fracture network and fractured reservoir. The attribute can clearly show the distribution and relative width of the fault damage zone that can be more than 1 km. The map showed branching faults and overlapping fault zones, with patchy patterns related to distributed fracturing along fault segments. The strength of the structural tensor attribute is consistent with the development of the fault damage zone which, in turn, is generally positively correlated with the width of fault damage zone. This has been evidenced by the fractured reservoirs from cores and logging data in the fault zone. In addition, micro-faults have a seismic response on the seismic section that could result in a variable response of the attribute. These are helpful for the seismic prediction of the fault damage zone in the Dengying Formation.

Although micro-faults are difficult to identify at depth, the envelope of the damage zone widening on the structure tensor attribute is usually caused by overlapping faults or branching faults. In this context, the width of the carbonate fault damage zone is related to fault size. In addition, permeable structures identified by the attributes are also greatly affected by karstification, lithology and lithofacies. These resulted in isolated, patchy seismic bodies that can hinder fault identification by conventional seismic attributes. In addition, the large distributed zones of strong attribute response in the southern part of Figure 7c are heavily karstified areas. These results are consistent with the power-law distribution of the fracture density's correlation with the distance to the fault damage zone [31]. There is generally one set of NWW-striking permeable structures along the fault damage zones, which are in line with the major fault zones (Figure 6). In addition, the attributes also show micro-faults of other orientations that are not consistent with major faults in the study area. These structures have been confirmed by well data that cannot be distinguished by conventional seismic attributes. The results of the fusion attribute by logging data constraints can directly characterize the distribution and strength of the permeable structures along fault damage zones. The width of damage zone increases towards the middle part of the segment, especially the width of the damage zone at the top of the fractured reservoirs. This may be related to fault overlapping and fault splay growth, and it may also be related to intense fracturing and karstification at the top of the carbonate reservoirs. The damage zone becomes complex with fault splays developing along the fault zone, which led to multi-stage superposition of fracturing with the development of the fractured reservoir. Away from the tip of fault damage zone, horsetail structures may also form a wide fractured reservoir block.

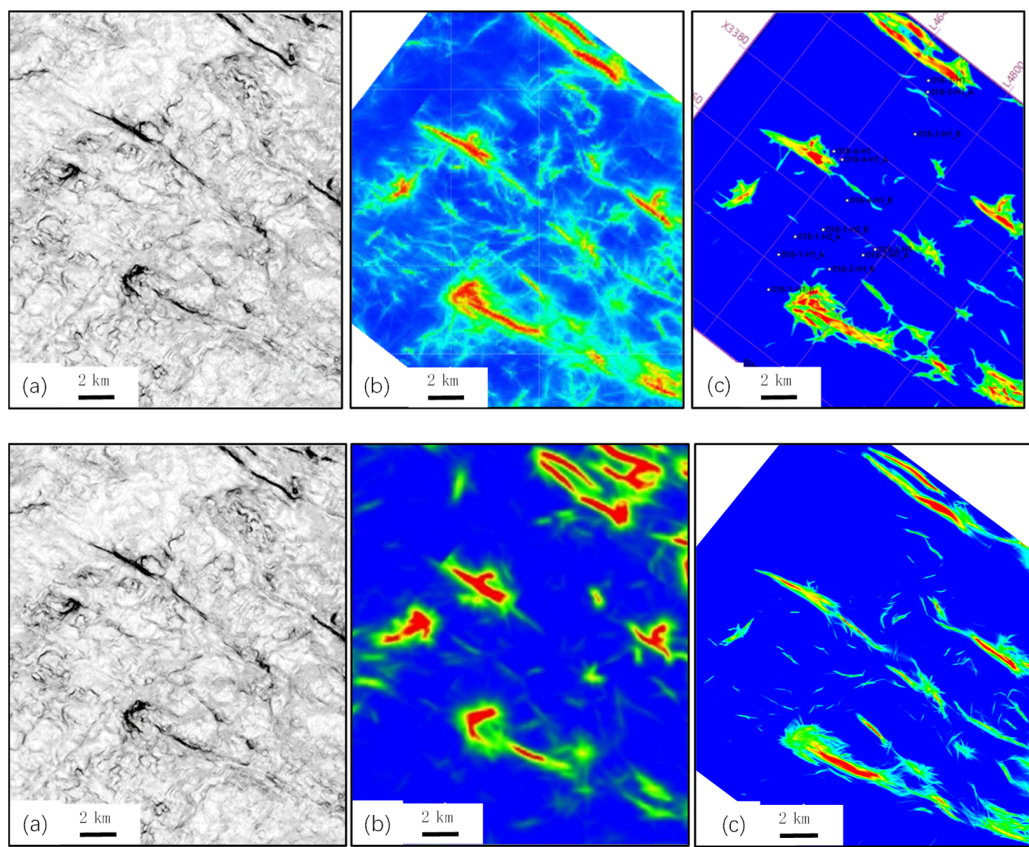


Figure 7. (a) Coherence, (b) seismic illumination and (c) fusion attribute of seismic illumination and structural tensor showing the NE-trending strike-slip fault damage zones in the Anyue Gasfield (the green envelope suggests the fault damage zone, and the orange-red blocks suggest the strong fractured zones).

4.2. Horizontal Well across the Strike-Slip Fault Damage Zone

Due to complicated fracture network and intense heterogeneous vug–cave assemblage in the deep fault damage zones, conventional seismic methods have difficulty in effectively describing the fracture network and the karst reservoirs [11]. Due to intense dissolution along the fault damage zone, the seismic attributes can be used to confine the fractured reservoirs. According to the statistical data, high-production wells are generally in strike-slip fault damage zones (Figure 8). The daily production of high-yield wells in strike-slip fault zones increases significantly with the decrease in the distance to the fault, which has an obvious power-law distribution to show the fracture effect on the gas production along the carbonate fault damage zone. Moreover, there are also many low-production wells that suggest sealed fracture zones in the fault zone. In this way, the seismic attribute can be a proxy of fractured reservoir prediction in the deep strike-slip fault zones, and it could significantly increase gas production along the fault damage zone. These provide optimized drilling targets and improve the drilling success rate.

Based on the seismic reservoir description, we carried out horizontal wells to penetrate the strike-slip fault zones for optimal reservoir units (Figures 7c and 9). According to the fault damage zone description in Anyue Gasfield, the gas enrichment zone was optimized by the overlap zone of the fault damage zone, the mound–shoal body and the karstic zone. Then, a fault segment was selected with a strong and wide fault damage zone from the seismic attributes, and a “sweet spot” of the fractured reservoir was selected. Together with the prediction of the fracture orientations and principal stress orientation, the target and wellbore trajectory were optimized across the strike-slip fault damage zone. For example, well MX-H2 gradually approaches the small NE-trending fault and had mud loss of 2954 m^3 ~250 m away from the fault core. There were four abnormal gas loggings in

10.5 m intervals and one gas invasion in a cumulative 553 m interval. This suggests that the well penetrated the fracture zone, although there is no seismic response in the seismic section and planar attributes. On the other hand, it indicates a wider fault damage zone in the fault zone. The fault to the northeast of the leakage point has intensified segmented activity, with large height difference and deformation and may develop a small fault on the west side, which is inferred to have been drilled to the outer damage zone of the fault zone. The recent four wells targeting the “sweet spots” in fractured reservoirs have obtained high production or penetrated better fractured reservoirs. These suggest that efficient well location characterized with “positive landform, abnormal seismic attribute in intense fault damage zone” is favorable for high-production wells.

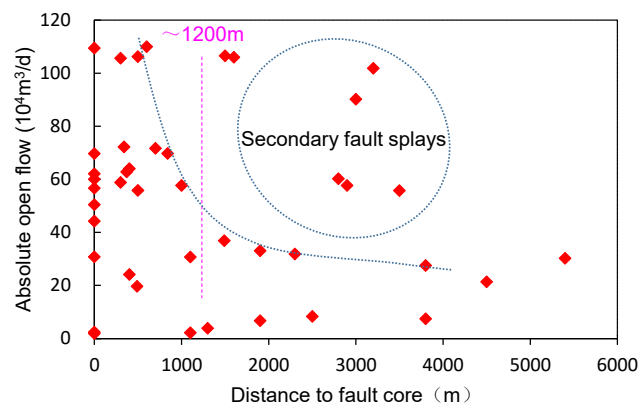


Figure 8. The absolute open flow of a gas well vs. distance to fault core at the fourth member of the Denying Formation in Anyue Gasfield.

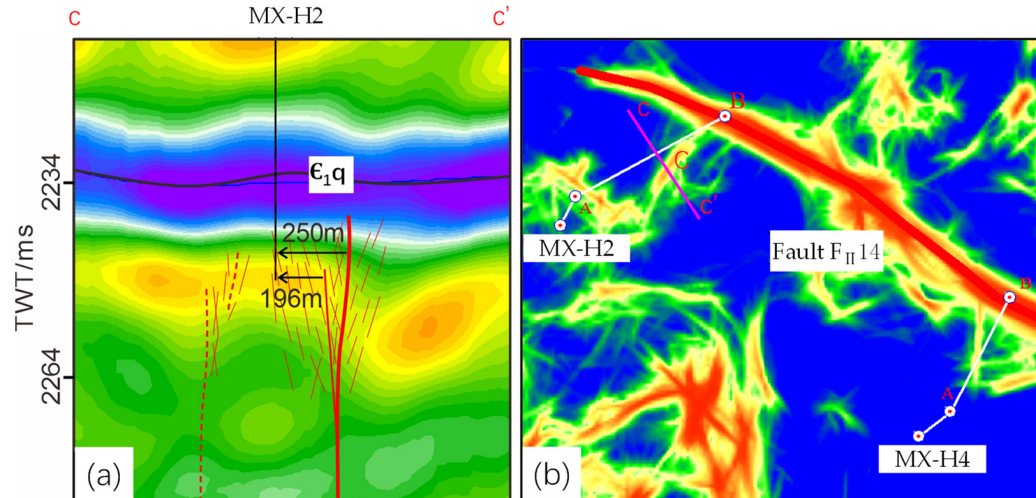


Figure 9. (a) Seismic section across the mud loss point of well MX-H2 (the well is 250 m far away to the major fault; E_1q : base of the Cambrian); (b) planar seismic illumination attribute showing the horizontal well locations at the fourth member of the Denying Formation in Anyue Gasfield (the horizontal interval from A to B; C: mud loss point).

5. Technology Challenges for Fractured Reservoir Exploitation

Due to the tight matrix reservoirs in the deep carbonates, fractured reservoirs are of significant importance in hydrocarbon exploitation in heterogeneous reservoirs [31–33]. The fracture network can enhance the permeability by 1–3 orders of magnitude and the fracture-related dissolution porosity by more than 20% in the deep tight reservoirs. In this way, the “sweet spot” of fractured reservoirs is the favorable target for economic production along the strike-slip fault damage zone. The fractured reservoir has been studied by geological, geophysical and engineering methods, of which the seismic technology plays an

important role in the reservoir description [32,33,36–38]. Owing to the intense heterogeneity of fractured reservoirs and low-resolution seismic data, there is still a big challenge in the description of fractured reservoirs in the deep subsurface.

With the seismic data by prestack time and depth migration process, the fault network and fault damage zone could be mapped by the seismic fault identification and fault damage zone description technologies in the Sichuan Basin (Figures 3–5 and 7). These integration techniques are applicable in deep tight matrix reservoirs. The accuracy of the planar fault identification and fault damage zone prediction can be compared with the advancements in the Tarim Basin [33,39]. Because of the low-density seismic acquisition with folds (<100) much less than the high-density acquisition (folds > 400) in the Tarim Basin, the seismic imaging of the strike-slip fault in seismic section is much better in the Tarim Basin. However, small strike-slip faults and fault segment linkages are ambiguous for seismic mapping in both basins. It is hard to identify the strike-slip fault without distinct seismic reflections of the fault surface (Figure 2) [18,19]. For this contribution, a high-density seismic survey could be carried out to retrieve better seismic data in strike-slip fault identification. The high-resolution seismic survey could be very helpful in strike-slip fault mapping [33,39]. Moreover, some strike-slip fault zones present continuous seismic reflection or kink shapes in seismic sections, which could be the pitfalls in fault interpretation [27]. In this way, the strike-slip fault identification and description techniques are of great importance in fault interpretation and mapping. Favorable seismic processing could be very helpful in this issue. Methods such as maximum likelihood can identify many small faults, although accompanied with the false images. These methods could be improved, and fusion with steerable pyramids could improve the seismic images of small faults and fault linkages.

Because the fracture cannot be discriminated by seismic data in the deep subsurface, the envelope of the fault damage zone could be a proxy for fracture imaging in the deep subsurface [31,33]. Moreover, there is still little understanding on the fracture network and its relation with the fractured reservoirs [32]. In addition, some weak fractured outer zones of the fault damage zone could not be imaged by the available seismic method (Figure 9b). These in turn constrain hydrocarbon exploitation from the deep fractured reservoirs. Methods such as illumination and structural tensor attributes could be improved to image the intense fractured reservoirs in the fault damage zone. Furthermore, new methods of development are expected to quantitatively or semiquantitatively evaluate the fracture network along the fault zone. With high-resolution 3D seismic data, most “bead shape” reflections have been successfully identified with fracture–cave reservoirs in the Tarim Basin [38–40]. The seismic description of small-scale vug and fracture reservoirs is still a big challenge in the exploitation of oil/gas in the deep subsurface. As the “sweet spots” of fractured reservoirs generally have some abnormal seismic responses along the fault damage zone (Figure 7), it could be helpful for the seismic description and well trajectory design. In this context, the seismic reservoir description technique cannot meet the requirements of well optimization along the fault zone. The advancement in seismic techniques is urgent for the description of fractured and matrix reservoir identification and the description of the deep subsurface.

Furthermore, the fracture sealing and connectivity of the fractured reservoirs are of greater difficulty in the deployment of horizontal wells [39,41]. The reliability of the fracture identification techniques requires further study and improvement. In addition, the reservoir connectivity along the fault damage zone urgently needs to be addressed during well deployment and oil/gas production [39–44]. With the complicated hydrocarbon migration and accumulation in the deep subsurface [45,46], the fracture network could be of great importance for the “sweet spot” reservoir exploitation in the petroliferous basin. The connectivity between the small vug–cave reservoirs has become more important for highly deviated and horizontal well employment to increase economical production from the deep subsurface. How to design highly deviated and horizontal well trajectories is an important issue in the description of fine reservoirs in the deep subsurface. In addition,

the large acid fracturing technique has been used and increased the gas production to a great extent. Moreover, many reservoirs are still difficult to obtain high production in. Some new methods such as sandy fracturing need further studies and experiments to increase gas production. The combination of techniques in different reservoirs is being applied to increase production, such as in fractured reservoirs by seismic quantitative identification and horizontal wells and matrix reservoirs by horizontal wells and large multiple fracturing operations. Due to the intense heterogeneity of the reservoirs and complicated fluid distribution, there are still big challenges, mainly involving the unstable production [47–49]. This exploitation practice in the Sichuan Basin provides new insights and techniques in the fractured reservoirs' development in the deep strike-slip fault zone.

6. Conclusions

Despite the complicated characteristics of the carbonate reservoirs and production in the deep Precambrian gasfield, we can propose the following conclusive points:

1. A favorable technology has been formed in strike-slip fault identification and mapping, including higher-resolution seismic data by prestack time and depth migration processing, a strike-slip fault identification method by planar and sectional marks, small strike-slip fault mapping by maximum likelihood and steerable pyramid attributes.
2. A fault damage zone description method is proposed by fusion attributes of seismic illumination and structural tensors, which is a favorable proxy for fractured reservoir prediction, and a large-scale fractured reservoir was found along the fault damage zone.
3. A large strike-slip fault system and its associated fault damage zone has been found in the central Sichuan Basin, which is favorable for fractured reservoir exploitation.
4. Horizontal well drilling across the strike-slip fault damage zone is proposed and found a new discovery on the “sweet spot” of a fractured reservoir along the fault damage zone.
5. New technologies are urgently needed for the economical exploitation of the deep fractured reservoirs in terms of seismic description and horizontal well drilling.

Author Contributions: Conceptualization, X.H. and G.G.; methodology, X.H., Q.T. and W.X.; software, B.M. and T.H.; investigation, Q.T. and G.W.; data curation, T.H. and W.T.; writing—original draft preparation, G.W. and W.X.; visualization, T.H. and W.T.; supervision, X.H. and G.G.; funding acquisition, X.H. and G.G. All authors have read and agreed to the published version of the manuscript.

Funding: The Science and Technology Cooperation Project of the CNPC-SWPU Innovation Alliance (2020CX010101) and the National Natural Science Foundation of China (41972121).

Data Availability Statement: Not applicable.

Acknowledgments: The authors are grateful to the editors and reviewers for their comments regarding manuscript improvement. We also thank Han Liang, Wenjun Luo, Chen Zhang and Puwei He for their help in the data process.

Conflicts of Interest: The authors declare no conflict of interest.

References

1. Zhang, G.; Wen, Z.; Liu, X.; Huang, T.; Wang, Z.; Yu, B.; Tong, X.; Li, Y.; Xin, R.; Chen, H.; et al. Evolution of global proto-type basin and the petroleum distribution. *Acta Pet. Sin.* **2020**, *41*, 1538–1554. (In Chinese with English Abstract)
2. Li, G.; Bai, G.P.; Gao, P.; Ma, S.H.; Chen, J.; Qiu, H.H. Geological characteristics and distribution of global primary hydrocarbon accumulations of Precambrian-Lower Cambrian. *Pet. Geol. Exp.* **2021**, *43*, 958–966. (In Chinese with English Abstract)
3. Craig, J.; Thurow, J.; Thusu, B. Global Neoproterozoic petroleum systems: The emerging potential in North Africa. *Geol. Soc. London Spec.* **2009**, *326*, 1–25. [[CrossRef](#)]
4. Bhat, G.M.; Craig, J.; Thurow, J.W.; Hakhoo, N.; Cozzi, A. Geology and Hydrocarbon Potential of Neoproterozoic-Cambrian Basins in Asia. *Geol. Soc. London Spec.* **2012**, *366*, 1–17. [[CrossRef](#)]
5. Grotzinger, J.; Al-Rawahi, Z. Depositional facies and platform architecture of microbialite-dominated carbonate reservoirs, Ediacaran-Cambrian Ara Group, Sultanate of OmanMicrobialite Reservoirs in Oman. *AAPG Bull.* **2014**, *98*, 1453–1494. [[CrossRef](#)]

6. Dou, L.R.; Wang, J.C.; Wang, R.C.; Wei, X.D.; Shrivastava, C. Precambrian basement reservoirs: Case study from the northern Bongor Basin, the Republic of Chad. *AAPG Bull.* **2018**, *102*, 1803–1824. [[CrossRef](#)]
7. Zhao, W.Z.; Wei, G.Q.; Yang, W.; Mo, W.L.; Xie, W.R.; Su, N.; Liu, M.C.; Zeng, F.Y.; Wu, S.J. Discovery of Wanyuan-Dazhou intracratonic rift and its exploration significance in the Sichuan basin, SW China. *Pet. Explor. Dev.* **2017**, *44*, 697–707. [[CrossRef](#)]
8. Guan, S.W.; Wu, L.; Ren, R.; Zhu, G.Y.; Peng, C.Q.; Zhao, W.T.; Li, J. Distribution of petroleum prospect of Precambrian rifts in main cratons, China. *J. Pet. Sci.* **2017**, *38*, 9–22.
9. Shen, A.J.; Chen, Y.A.; Zhang, J.Y.; Ni, X.F.; Zhou, J.G.; Wu, X.N. Characteristics of intra-platform rift in ancient small-scale cratonic platform of China and its implications for hydrocarbon exploration. *Oil Gas Geol.* **2020**, *41*, 15–25. (In Chinese with English Abstract)
10. Xie, J. Innovation and practice of the key technologies for the efficient development of the supergiant Anyue gas field. *Nat. Gas Industry* **2020**, *40*, 1–10. [[CrossRef](#)]
11. Lin, Y.C.; Li, C.M.; Gu, W.; Luo, W.J.; Wang, Z.Y.; Yu, Z.; Zhang, J.; Bie, J.; Li, W.Q. Seismic fine characterization of deep carbonate fractured-vuggy reservoir: Case study of the 4th Member of Sinian Dengying Formation in Anyue Gas Field, Sichuan Basin. *Nat. Gas Geosci.* **2020**, *31*, 1792–1801.
12. Zhou, Y.; Yang, F.L.; Jia, Y.L.; Zhou, X.F.; Zhang, C.H. Characteristics and controlling factors of dolomite karst reservoirs of the Sinian Dengying Formation, central Sichuan Basin, southwestern China. *Precambrian Res.* **2020**, *343*. [[CrossRef](#)]
13. Feng, Q.F.; Xiao, Y.X.; Hou, X.L.; Chen, H.K.; Wang, Z.C.; Feng, Z.; Tian, H.; Jiang, H. Logging identification method of depositional facies in Sinian Dengying Formation of the Sichuan Basin. *Pet. Sci.* **2021**, *18*, 1086–1096. [[CrossRef](#)]
14. Wang, Y.; Wang, S.Y.; Yan, H.J.; Zhang, Y.J.; Li, J.Z.; Ma, D.B. Microbial carbonate sequence architecture and depositional environments of Member IV of the Late Ediacaran Dengying Formation, Gaoshiti–Moxi area, Sichuan Basin, Southwest China. *Geol. J.* **2021**, *56*, 3992–4015. [[CrossRef](#)]
15. Shan, X.Q.; Zhang, J.; Zhang, B.M.; Liu, J.J.; Zhou, H.; Wang, Y.J.; Fu, Z.W. Characteristics of dolomite karstic reservoir in the Sinian Dengying Formation, Sichuan Basin. *Petrol. Res.* **2017**, *2*, 13–24. [[CrossRef](#)]
16. Zhou, Z.; Wang, X.Z.; Yin, G.; Yuan, S.S.; Zeng, S.J. Characteristics and genesis of the (Sinian) Dengying Formation reservoir in Central Sichuan, China. *J. Nat. Gas Sci. Eng.* **2016**, *29*, 311–321. [[CrossRef](#)]
17. Luo, B.; Yang, Y.M.; Luo, W.J.; Wen, L.; Wang, W.Z.; Chen, K. Controlling factors of Dengying Formation reservoirs in the central Sichuan paleo-uplift. *Petrol. Res.* **2017**, *2*, 54–63. [[CrossRef](#)]
18. Ma, D.B.; Wang, Z.C.; Duan, S.F.; Gao, J.R.; Jiang, Q.C.; Jiang, H.; Zeng, F.Y.; Lu, W.H. Structural characteristics of strike slip faults and significance of natural gas accumulation in Gaoshiti Moxi area, Sichuan Basin. *Pet. Explor. Dev.* **2018**, *45*, 795–805. [[CrossRef](#)]
19. Jiao, F.; Yang, Y.; Ran, Q.; Wu, G.; Liang, H. Distribution and gas exploration of the strike-slip faults in the central Sichuan Basin. *Nat. Gas Ind. B* **2021**, *41*, 59–68. (In Chinese with English Abstract) [[CrossRef](#)]
20. Wen, L.; Ran, Q.; Tian, W.; Liang, H.; Zhong, Y.; Zou, Y.; Su, C.; Wu, G. Strike-Slip Fault Effects on Diversity of the Ediacaran Mound-shoal Distribution in the Central Sichuan Intracratonic Basin, China. *Energies* **2022**, *15*, 5910. [[CrossRef](#)]
21. He, D.; Li, D.; Zhang, G.; Zhao, L.; Fan, C.; Lu, R.; Wen, Z. Formation and evolution of multi-cycle superposed Sichuan Basin, China. *Chin. J. Geol.* **2011**, *46*, 589–606. (In Chinese with English Abstract)
22. Li, H.K.; Li, Z.Q.; Long, W.; Wan, S.S.; Ding, X.; Wang, S.Z.; Wang, Q.Z. Vertical configuration of Sichuan Basin and its superimposed characteristics of the prototype basin. *J. Chengdu Univ. Technol.* **2019**, *46*, 257–267. (In Chinese with English Abstract)
23. Yang, Y.M.; Yang, Y.; Yang, G.; Song, J.R.; Wen, L.; Deng, C.G.; Xia, M.L.; Ran, Q.; Duan, G.B.; Luo, B.; et al. Gas accumulation conditions and key technologies for exploration & development of Sinian and Cambrian gas reservoirs in Anyue gasfield. *Pet. Res.* **2018**, *3*, 221–238.
24. Zou, C.N.; Du, J.H.; Xu, C.C.; Wang, Z.C.; Zhang, B.M.; Wei, G.Q.; Wang, T.S.; Yao, G.S.; Deng, S.H.; Liu, J.J.; et al. Formation, distribution, resource potential and discovery of the Sinian–Cambrian giant gas field, Sichuan Basin, SW China. *Petrol. Explor. Dev.* **2014**, *41*, 306–325. [[CrossRef](#)]
25. Wei, G.Q.; Wang, Z.H.; Li, J.; Yang, W.; Xie, Z.Y. Characteristics of source rocks, resource potential and exploration direction of Sinian-Cambrian in Sichuan Basin, China. *J. Nat. Gas Geosci.* **2017**, *2*, 289–302. [[CrossRef](#)]
26. Zhang, G.R.; Liao, Q.; Yu, Y.; Ran, Q.; Xiao, Y.; Lu, G.Y.; Li, X.M.; Liang, H.; Zeng, M. Seismic prediction on the favorable efficient development areas of the Longwang-miao Fm gas reservoir in the Gaoshiti-Moxi area, Sichuan Basin. *Nat. Gas Ind.* **2017**, *27*, 66–75. (In Chinese with English Abstract)
27. Harding, T.P. Identification of wrench fault using subsurface structural data: Criteria and pitfalls. *AAPG Bull.* **1990**, *74*, 1090–1609.
28. Ma, D.B.; Zhao, Y.M.; Zhang, Y.T.; Yang, P.F.; Yang, M.; Li, L. Application of maximum likelihood attribute to fault identification: A case study of Rewapu block in Halahatang area, Tarim Basin, NW China. *Nat. Gas Geosci.* **2018**, *29*, 817–825. (In Chinese with English Abstract)
29. Mathewson, J.M.; Hale, D. Detection of channels in seismic images using the steerable pyramid. In Proceedings of the 2008 SEG Annual Meeting, Las Vegas, NV, USA, 9 November 2008; pp. 859–863.
30. Song, Y.T.; Wu, G.H.; Tian, W.Z.; Xu, Y.G.; Ma, B.S. Application of Navigation Pyramid technology in the identification of strike-slip faults in Gaomo Area, Sichuan Basin. *Chem. Engin. Design Comm.* **2022**, *48*, 19–20+174. (In Chinese with English Abstract)
31. Wu, G.H.; Gao, L.H.; Zhang, Y.T.; Ning, C.Z.; Xie, E. Fracture attributes in reservoir-scale carbonate fault damage zones and implications for damage zone width and growth in the deep subsurface. *J. Struct. Geol.* **2019**, *118*, 181–193. [[CrossRef](#)]

32. Babasafari, A.A.; Chinelatto, G.F.; Vidal, A.C. Fault and fracture study by incorporating borehole image logs and supervised neural network applied to the 3D seismic attributes: A case study of pre-salt carbonate reservoir, Santos Basin, Brazil. *Pet. Sci. Technol.* **2022**, *40*, 1492–1511. [[CrossRef](#)]
33. Wang, R.J.; Yang, J.P.; Chang, L.J.; Zhang, Y.T.; Sun, C.; Wu, G.H.; Bai, B.C. 3D modeling of fracture-cave reservoir from an ultra-depth strike-slip fault-controlled carbonate oilfield in Northwestern China. *Energies* **2022**, *15*, 6415. [[CrossRef](#)]
34. Xie, X.B.; Jin, S.W.; Wu, R.S. Wave-equation-based seismic illumination analysis. *Geophysics* **2006**, *71*, 169–177. [[CrossRef](#)]
35. Xu, J.L.; Zhou, D.H.; Wang, Y.Y.; Bian, L.E.; Lv, Z.Y. Forward analysis of the influencing factors in prestack time migration imaging of fault surface waves based on the staggered-grid finite-difference method. *Chin. J. Geophys.* **2018**, *61*, 733–741.
36. Ou, C.H.; Li, C.C.; Huang, S.Y.; Lu, W.T.; Sheng, J.J.; Xiong, H.L. Three-dimensional discrete network modeling of structural fractures based on the geometric restoration of structure surface: Methodology and its application. *J. Pet. Sci. Engin.* **2018**, *161*, 417–426. [[CrossRef](#)]
37. Benmadi, M.; Sayantan, G.; Roger, S.; Kurt, M.; Mashhad, F. Practical aspects of upscaling geocellular geological models for reservoir fluid flow simulations: A case study in integrating geology, geophysics, and petroleum engineering multiscale data from the Hunton Group. *Energies* **2020**, *13*, 1604.
38. Li, X.; Li, J.; Li, L.; Wan, Z.; Liu, Y.; Ma, P.; Zhang, M. Seismic wave field anomaly identification of ultra-deep heterogeneous fractured-vuggy reservoirs: A case study in Tarim Basin, China. *Appl. Sci.* **2021**, *11*, 11802. [[CrossRef](#)]
39. Wang, Q.H.; Zhang, Y.T.; Xie, Z.; Zhao, Y.W.; Zhang, C.; Sun, C.; Wu, G.H. The Advance and challenge of seismic technique on the ultra-deep carbonate reservoir exploitation in the Tarim Basin, Western China. *Energies*, **2022**; *in press*.
40. Lu, X.B.; Wang, Y.; Yang, D.B.; Wang, X. Characterization of paleo-karst reservoir and faulted karst reservoir in Tahe Oilfield, Tarim Basin, China. *Adv. Geo-Energy Res.* **2020**, *4*, 339–348. [[CrossRef](#)]
41. Zhu, W.W.; He, X.P.; Khirevich, S.; Patzek, T.W. Fracture sealing and its impact on the percolation of subsurface fracture networks. *J. Pet. Sci. Engin.* **2022**, *218*. [[CrossRef](#)]
42. He, X.; Wang, R.; Yang, J.; Li, S.; Yan, C.; Wu, G. Optimization of oil productivity from the ultra-depth strike-slip fault-controlled carbonate reservoirs in northwestern China. *Energies* **2022**, *15*, 3472. [[CrossRef](#)]
43. Yang, X.W.; Wang, R.J.; Deng, X.L.; Li, S.Y.; Zhang, H.; Yao, C. Theoretical exploration and practice of water injection gravity flooding oil in ultra-deep fault-controlled fractured-cavity carbonate reservoirs. *Pet. Explor. Dev.* **2022**, *49*, 133–143. [[CrossRef](#)]
44. Shen, F.X.; Li, S.Y.; Deng, X.L.; Liu, Z.L.; Guo, P.; Wu, G.H. Application of EOR using water injection in carbonate condensate reservoirs in the Tarim Basin. *Energies* **2022**, *15*, 3881. [[CrossRef](#)]
45. He, Z.T.; Yin, X.D.; Jiang, S.; Lei, M.Z.; Liu, Y.; Zhao, R.Q.; Zhu, B.Q. Source rock classification, maturity and their implications in paleoenvironment reconstruction in the Zhu III sub-basin, China. *J. Pet. Sci. Engin.* **2022**, *216*. [[CrossRef](#)]
46. Zhu, Y.F.; Zhang, Y.T.; Zhao, X.X.; Xie, Z.; Wu, G.H.; Li, T.; Yang, S.; Kang, P.F. The fault effects on the oil migration in the ultra-deep Fuman Oilfield of the Tarim Basin, NW China. *Energies* **2022**, *15*, 5789. [[CrossRef](#)]
47. Yao, G.S.; Wu, X.Z.; Sun, Z.D.; Yu, C.H.; Ge, Y.H.; Yang, X.Y.; Wen, L.; Ni, C.; Fu, X.D.; Zhang, J.Y. Status and prospects of exploration and exploitation key technologies of the deep oil & gas resources in onshore China. *Nat. Gas Geosci.* **2017**, *28*, 1154–1164. (In Chinese with English Abstract)
48. Ma, Y.; Li, M.; Cai, X.; Xu, X.; Hu, D.; Qu, S.; Li, G.; He, D.; Xiao, X.; Zeng, Y.; et al. Mechanisms and exploitation of deep marine petroleum accumulations in China: Advances, technological bottlenecks and basic scientific problems. *Oil Gas Geol.* **2020**, *41*, 655–672. (In Chinese with English Abstract)
49. Wang, H.; Kou, Z.H.; Bagdonas, D.A.; Phillips, E.H.W.; Alvarado, V.; Johnson, A.C.; Jiao, Z.S.; McLaughlin, J.F.; Quillinan, S.A. Multiscale petrophysical characterization and flow unit classification of the Minnelusa eolian sandstones. *J. Hydrol.* **2022**, *607*. [[CrossRef](#)]